

RF DEFLECTOR FOR BUNCH LENGTH MEASUREMENT AT LOW ENERGY AT PSI

A. Falone, H. Fitze, R. Ischebeck, Y. Kim, M. Pedrozzi, V. Schlott, B. Steffen, L. Stingelin, PSI, Villigen, Switzerland

D. Alesini, L. Ficcadenti, L. Palumbo, INFN-LNF, Frascati, Italy

Abstract

RF deflectors are crucial diagnostic tools for bunch length and slice emittance measurements with sub-picoseconds resolution. Their use is essential in commissioning and operation of VUV and X-ray FELs. The 250MeV FEL injector [1], under construction at PSI, will use two RF deflectors. The first one will be installed after the gun at low energy ($\sim 7\text{MeV}$), the second one at the end of the Linac at high energy (250MeV). While multi cell deflectors are used at high beam energy [2]; at low energy, where space constraints are quite stringent and voltage requirements are more relaxed, a single cell cavity is the preferable option.

The first RF deflector (which is presented in this paper) consists of a single cell standing wave cavity tuned at 2997.912MHz (frequency of the Linac S-band structures). Sophisticated methods to reconstruct the bunch temporal profile and the slice emittance after the gun can be implemented by using this cavity [3]. With the use of a spectrometer beam line it would then be possible to reconstruct the whole beam phase space (transverse and longitudinal) in the gun region.

RF DESIGN

The RF design has been done jointly by Paul Scherrer Institut and INFN (Istituto Nazionale di Fisica Nucleare, Italy). The mechanical design and manufacturing is under responsibility of INFN. Several constraints played a role in the choice of the geometry: space available, power source available, cost, time needed for production. A single cell pillbox cavity tuned at 2997.912MHz is the best compromise within these constraints.

The deflecting mode in a pure pillbox cavity is the TM_{110} , but iris and beam pipes induce a perturbation of this mode as consequence a transverse electric field appears on the beam pipe region (see figure 1). In figure 1 and 2 the HFSS model (half structure) of this cavity and the electric and magnetic field are presented, and in table 1 the main RF parameters obtained from HFSS are listed.

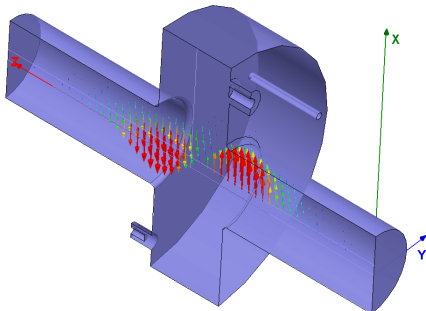


Figure 1: HFSS Half cell and E_x field.

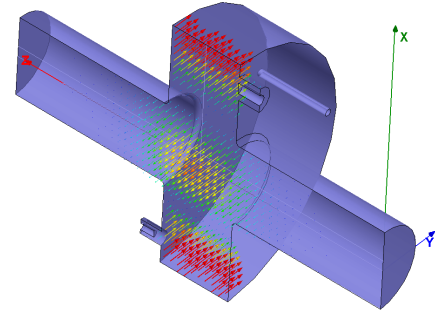


Figure 2: HFSS Half cell and H_y field.

Table 1: Main RF Parameters

| Parameter | Value | Unit |
|------------------------------------|------------|--------------------|
| No. Cells | 1 | - |
| Frequency | 2997.9 | MHz |
| Rep.Rate | ≤ 10 | Hz |
| Quality Factor Unloaded – Q_0 | 15800 | - |
| Quality Factor Loaded – Q_L | 7500 | - |
| Coupling Factor – β | 1.09 | - |
| Transverse Impedance – R_{\perp} | 0.53 | $\text{M}\Omega$ |
| Length (Flange to flange) | 0.1 | m |
| Max. Input power | 25 | kW |
| Filling time | ~ 0.8 | μs |
| Aperture Beam pipe (diameter) | 38 | mm |
| Working temperature | 40 | $^{\circ}\text{C}$ |

The amplitude of the transverse deflecting voltage acting on an ultra-relativistic beam passing through the cavity on axis is:

$$V_{\perp} = \left| \int_0^L [cB_{\perp}(z) - jE_{\perp}(z)] \cdot e^{jkz} \cdot dz \right| \quad (1)$$

According with equation 1 the transverse shunt impedance is then given by:

$$R_{\perp} = \frac{V_{\perp}^2}{2P_{\text{diss}}} \quad (2)$$

where P_{diss} is the power dissipated. Alternatively, one can use the Panofsky-Wenzel theorem using the longitudinal electric field at a certain distance r_0 from the axis [4]:

$$R_{\perp} = \frac{\left| \int_0^L E_z(r_0) \cdot e^{jkz} dz \right|^2}{2P_{\text{diss}} \cdot (kr_0)^2} \quad (3)$$

The length of the cavity has been chosen to maximize the transverse shunt impedance. In figure 3 the transverse shunt impedance as function of the cavity length is plotted.

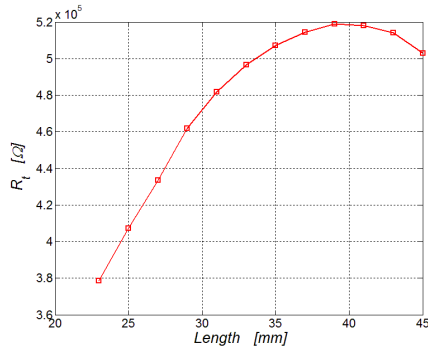


Figure 3: Transverse shunt impedance as function of the cavity length.

The cavity is fed by a small klystron (25kW maximum output power, pulsed at 10Hz) through a coaxial high power input coupler. The S_{11} around the working frequency is plotted in figure 4.

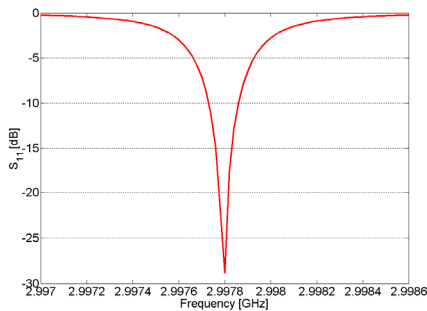


Figure 4: S_{11} around the working frequency.

The deflecting mode has two polarizations (horizontal and vertical). The cavity will be used only for vertical deflection; the orthogonal polarization is then shifted by means of two small rods (3mm diameter) which give a frequency shift of 45.8MHz. The cavity is provided with a small tuner placed 45° respect the vertical deflection plane to avoid field perturbations around the pickup. In this configuration it allows a frequency correction of 550kHz/mm which is sufficient for compensating manufacturing errors; a further tuning will be done by adjusting the operating temperature by means of a dedicated cooling circuit. The temperature is then stabilized within 0.1°C. Finally the cavity is provided with a coaxial pickup with a coupling factor of -30dB.

Other Modes

Lower and higher order modes have been investigated. In table 2 the closer modes are listed with the main parameters. The orthogonal mode resonates at 3.0473GHz due to the rods perturbations; other modes coupled with the beam are the dipole one at 3.945GHz, and the TM_{010} fundamental one at 2.045GHz.

Table 2: Other resonant modes

| f_0 [GHz] | Q_0 | Rs/Q [Ω] | Mode |
|-------------|-------|------------|---------------------------------------|
| 2.045 | 13700 | 29.2 | TM_{010} – Accelerating |
| 2.997 | 15800 | 33.5 | TM_{110} – Deflecting working mode |
| 3.047 | 15100 | 34.1 | TM_{110} – Orthogonal polarization |
| 3.945 | 14200 | 7.3 | Dipole mode interacting with the beam |

Wakefield effects are still under investigations.

ASTRA AND GPT SIMULATIONS

GPT [5] and ASTRA simulations have been performed to crosscheck bunch length and slice emittance measurements. For different bunch charge options the beam has been tracked from cathode up to a screen located 1.6m downstream the cavity (see fig.5). The beam line, where the measurements will take place, is sketched in figure 5. It consists of a triplet of quadrupoles, a dipole magnet to bend the beam towards the spectrometer line, and two fluorescent screens to measure the beam size.

With the use of the deflector also slice energy spread measurements can be implemented ([2] and [3]).

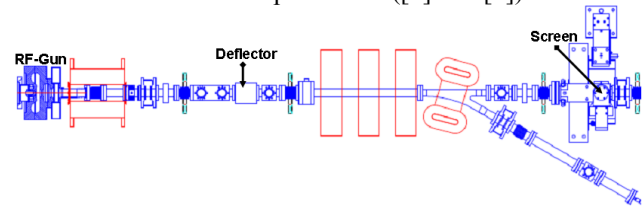


Figure 5: Layout of the Gun region.

Simulations have been divided in two parts: first the beam has been tracked from the gun up to the deflector entrance using ASTRA; then GPT has been used to track the beam from the deflector entrance up to the screen, since it is suited for modeling RF transverse fields. In the simulations the quadrupoles have been switched off. In table 3 the main beam parameters at the deflector entrance. The longitudinal distribution at the deflector entrance is rectangular with rise and fall time of 0.7ps.

Table 3: Main beam parameters at the deflector entrance

| Parameter | Q=10 pC | Q=200 pC |
|----------------------------------|---------------------|---------------------|
| Energy – E | 6.56 MeV | 6.56 MeV |
| Emittance – ϵ | 0.147 μm | 0.705 μm |
| Beam size – σ | 0.46 mm | 1.17 mm |
| Beta Functions – β | 20 m | 27 m |
| Bunch length (FWHM) – Δz | 1.0 mm | 2.5 mm |
| Bunch length (FWHM) – Δt | 3.34 ps | 8.30 ps |

Usually the effect of a deflecting cavity is sketched as follow (see figure 6):

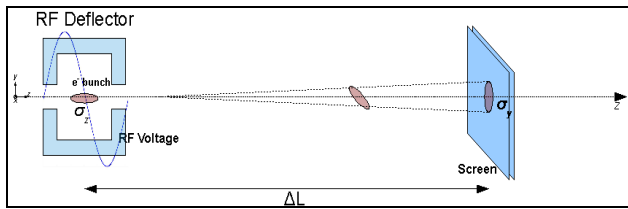


Figure 6: Sketch of the beam deflection due to a deflecting cavity.

When the beam passes through the cavity at the zero crossing phase, and taking into account the effect of the finite transverse emittance, we have that the beam size at the screen $\sigma_{y,S,\epsilon}$ is related to the bunch length [3] at the deflector position, according to equation 4:

$$\sigma_{y,S,\epsilon} = \sqrt{\frac{\epsilon_N \beta_S}{\gamma} + \left[\frac{eV_{\perp}}{E} \sigma_z \left[\frac{\omega}{c} \cos \phi_{RF} \right] \sqrt{\beta_D \beta_S} \cdot \sin(\Delta\psi_{DS}) \right]^2} \quad (4)$$

Where β_D and β_S are the beta functions at the deflector and screen position respectively, V_{\perp} is the transverse deflecting voltage and $\Delta\psi_{DS}$ is the phase advance between deflector and screen. Due to the relative low energy space charge effects have been taken into account. The resolution length, i.e. the minimum slice length that can be measured, is given by:

$$L_{res} = \frac{c E/e}{\omega \cdot V_{\perp}} \cdot \frac{\sqrt{\epsilon_N/\gamma}}{\sqrt{\beta_D} \cdot \sin \Delta\psi_{DS}} \quad (5)$$

Resolution length and number of slices as function of the deflecting voltage are plotted in figure 7.

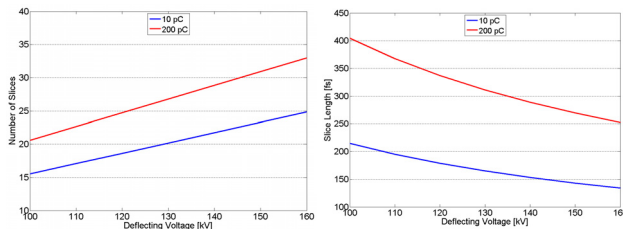


Figure 7: Slice length and number of slices as function of the deflecting voltage.

Even in the shortest bunch case the number of slices (~ 25) is sufficient to characterize properly the beam in the gun region. In figure 8 the transverse profile (from GPT simulations) of the beam at the screen position without and with RF applied is presented for the 200pC beam and 160kV deflecting voltage (25kW input power).

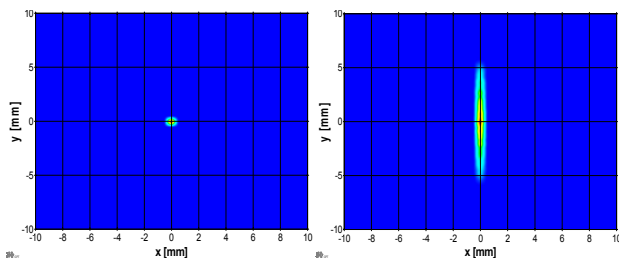


Figure 8: Transverse charge distribution without and with 160kV deflecting voltage applied for a 200pC beam at the screen position.

DIAGNOSTIC SETUP

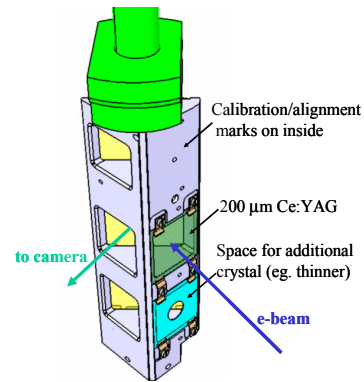


Figure 9: CAD drawing of the low energy screen holder.

The profiles of the deflected beam are visualized by a YAG:Ce crystal and imaged on a CCD detector. The fluorescent crystal is aligned for normal incidence angle of the electron bunches, while a mirror reflects the light out of the UHV chamber, where the operator can select between overview and high resolution imaging. Both optical paths are equipped with commercial CCD cameras and objectives. The overview path will be used during initial commissioning and machine set-up, providing a field of view of $37 \times 28 \text{ mm}^2$. The high-resolution path images only the central part of the crystal ($9 \times 7 \text{ mm}^2$) and has been designed for an optical resolution of $\sim 10 \mu\text{m}$. For an improved signal to noise ratio, which might be required for the low charge (10 pC) operation mode, cooled CCD and room-temperature CMOS cameras are currently under evaluation. An identical set-up will be mounted in the low energy dispersive arm to allow for sliced energy spread measurements.

CONCLUSIONS

Beam dynamics studies confirmed that the single cell deflector can properly measure bunch length and slice emittance with sufficient resolution (~ 25 slices for a 10pC beam) even in the shortest bunch case. The mechanical design is now in progress. The RF deflector will be installed and in operation during the first phase of the 250MeV FEL injector commissioning (January 2010).

REFERENCES

- [1] A.Oppelt et al., "Towards a low emittance X-Ray FEL at PSI", Proceeding FEL Conference 2007, Novosibirsk, Russia.
- [2] D.Alesini et al., "RF Deflector design and measurements for the longitudinal and transverse emittance at SPARC", Nucl.Instr.& Meth.,A568 (2006) 488.
- [3] P.Emma et al., "A Transverse RF Deflecting structure for bunch length and phase space diagnostic", LCLS-TN-00-12, Aug. 2000
- [4] Li, Corlett, "RF Deflecting cavity design for Berkeley Ultrafast X-Ray source", Proceeding EPAC02, Paris, France.
- [5] www.pulsar.nl